Polymer Bulletin 56, 63–74 (2006)
DOI 10.1007/s00289-005-0462-6

Polymer Bulletin

Poly(amidoamine) Dendrimers Bearing Electron-Donating Chromophores: Fluorescence and Electrochemical Properties

Bing-Bing Wang[a], Xin Zhang[a], Ling Yang[a], Xin-Ru Jia (✉)[a], Yan Ji[a], Wu-Song Li[a], Yen Wei (✉)[b]

[a] Department of Polymer Science & Engineering, College of Chemistry & Molecular Engineering, Peking University, Beijing 100871 China
Fax: 86-10-62751708; E-mail: xrjia@pku.edu.cn

[b] Department of Chemistry, Drexel University, Philadelphia, PA 19104 USA
Fax: 215-895-1265; E-mail: weiyen@drexel.edu

Received: 4 August 2005 / Revised version: 7 October 2005 / Accepted: 17 October 2005
Published online: 9 November 2005 –

Electronic Supplementary Material: Supplementary material is available in the online version of this article at http://dx.doi.org/10.1007/s00289-005-0462-6

Summary

Poly(amidoamine) dendrimers from the zeroth generation (G 0) to the fifth generation (G 5) bearing electron-donating chromophores, i.e. *N*, *N*-dimethylphenylamine (PA), carbazole (Cz) and pyrene (Py) chromophores have been synthesized. The macromolecular reactions of chromophoric modifications of PAMAM dendrimers were monitored by fluorescence spectroscopy. The reliability of fluorescence monitoring was confirmed by NMR spectroscopy. Compared with widely applied environment-sensitive fluorescence probe techniques, a distinct feature of the fluorescence monitoring was that it directly reflected the conversion of chemical bonds. A comparative study revealed that the fluorescence quenching of small molecular Py by the high generation dendrimers of PAMAM-PA was a static quenching process. The high generation dendrimers of PAMAM-Py possessed relatively compact Py shells as compared with the same generation PAMAM-PA. Electrochemical studies revealed an architectural transition occurring from an open and flexible structure to a closely packed globular structure between G 2 and G 3. The electron-donating ability of PAMAM-PA was affected by dendritic architectures.

Introduction

In recent years, the synthesis and related properties of a new class of tree-like macromolecules called as dendrimers have attracted much attention. Various functionalized dendrimers with unique properties can be designed and tailored by covalently attaching functional components to the exterior, interior or branches of dendrimers [1]. A large number of papers have reported the synthesis and properties of dendrimers bearing various moieties, such as dansyl sulfonate [2], azobenzene [3],

cumarin [4] and porphyrins chromophores [5]. In general, these modified dendrimers were found to possess interesting properties and functions. As examples, Crooks and Baker [6] synthesized the poly (propylene imine) dendrimers modified with pyrene (Py) chromophores and found the correlation of spectroscopic properties with dendrimer structures. Fox and co-workers [7] reported on the fluorescence resonance energy transfer of polyether dendrons bearing Py and naphthalene chromophores. Abruna [8] et al. explored the electrochemical properties of poly (amidoamine) (PAMAM) dendrimers modified with polypyridine groups.

On the other hand, the reaction monitoring of the modification process of dendrimers was well known to play an important role in tailoring and optimizing the properties and related functions of dendrimers bearing chromophores. Recently, several research groups such as Kim [13], Yilmaz [14], Scaiano [15], and Mullen [16] have reported on online monitoring of polymerization process or the photoisomerization of azobenzene groups by UV-vis and fluorescence spectroscopy.

We have had a long-standing interest in the synthesis, photochemical and photo-physical properties, functionalization of dendrimers and their potential applications [9, 10, 11, 12]. In our previous work, we reported that PAMAM dendrimers bearing photosensitive chromophores could be fabricated into photo-responsive ultrathin films, which could be further stabilized by changing non-covalent linkage into covalent linkage between layers after UV light irradiation [9, 10].

In this article, we described the peripheral modification of PAMAM dendrimers with *N*, *N*-dimethylphenylamine (PA), carbazole and pyrene (Py) chromophores (Scheme 1), and their fluorescence and electrochemical properties were explored. Furthermore, a fluorescence approach was applied to monitor the functionalization reaction process of macromolecular dendrimers.

Experimental Parts

Materials

N-(1-pyrenyl)maleimide was purchased from Aldrich. Bu_4NPF_6 was purchased from Fluka Co. All other chemicals were purchased from Beijing Chemicals Co. Poly(amidoamine) (PAMAM) dendrimers from the zeroth (G 0) to the fifth generations (G 5) were synthesized according to the literature [17] and further purified by dialysis membranes (MW 12,000 for G 4 and G 5, MW 5,000 for G 3, MW 3,000 for G 2 and MW 1,000 for G 1) using methanol as a solvent. The chemical structures of PAMAM dendrimers were confirmed by ^{1}H-NMR and FT-IR according to the literature [17]. Benzaldehyde was purified by distillation under reduced pressure. Methanol was purified by refluxing over magnesium bits followed by distillation. *N*, *N*-dimethylformamide, 4-dimethylamino-benzaldehyde, ethanol, chloroform and ethyl ether were purified according to the standard procedures.

Measurements

UV-vis spectra were acquired on a UV-vis scanning spectrophotometer (Schimaduza UV-2101 PC) at room temperature. ^{1}H-NMR spectra were obtained on a Varian Mercury 200MHz or 300MHz NMR spectrometer at room temperature using chloroform-*d*, methanol-d_4, acetone-d_6 or dimethyl-d_6 sulfoxide as solvents and tetramethylsilane as

an internal standard. FT-IR spectra were acquired on a Nicolet Magna IR-750 spectrometer in a KBr pellet form. The fluorescence emission measurements were carried out at room temperature in methanol using a Hitachi F-4500 fluorescence spectrophotometer. The slit width of both monochromators was 5.0 nm. Cyclic-voltammetry was performed with a computer-controlled EG&G Instrument (PAR) in a three-electrode single-compartment cell with acetonitrile (5 mL) as solvent, tetrabutyl-ammonium hexafluorophosphate (0.1M Bu_4NBF_6) as the supporting electrolyte, and using a platinum disk (0.5 mm diameter) as the working electrode, a platinum wire as the counter electrode and a Ag/AgCl wire as the reference electrode. The solution ([chromophore]=1.0×10^{-2} M) was purged with N_2 for 10 min before each measurement.

Scheme 1. Peripheral modification of poly(amidoamine) dendrimers G 0 to G 5 with benzaldehyde, 4-dimethylaminobenzaldehyde, 9-(3-bromopropyl)-9H-carbazole, *N*-(1-pyrenyl) maleimide.[a]

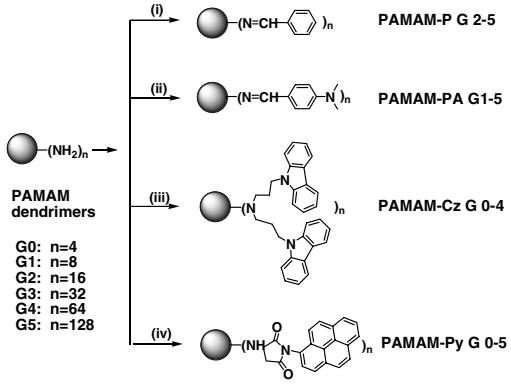

[a]Reagents and conditions: (i): Benzaldehyde, Na_2SO_4, methanol, 60ºC, 12 h; (ii):4-Dimethyl-aminobenzaldehyde, Na_2SO_4, methanol, room temperature, 24 h; (iii): 9-(3-bromopropyl)-9H-carbazole, *N, N*-dimethylformamide, 30ºC, 12 h; (iv): *N*-(1-pyrenyl)maleimide, acetone, room temperature, 24 h.

Synthesis of PAMAM Dendrimers Bearing N, N-Dimethylphenylamine (PAMAM-PA G 1, G 2, G 3, G 4 and G 5)

PAMAM-PA G 1. 4-Dimethylaminobenzaldehyde (0.70 g, 6.6 mmol) and anhydrous sodium sulfate (1.0 g) were added to the methanol solution (30 mL) of PAMAM G 1 (0.050 g, 0.010 mmol). The mixture was subsequently stirred at room temperature for 24 h. The solvent was removed under a reduced pressure. The residue was dissolved in chloroform (5 mL) and filtrated. The filtrate was then concentrated under a reduced pressure. The resulting crude product was dissolved in methanol (5 mL) and dropped into anhydrous ether (100 mL) with vigorous stirring. The precipitate was collected and further purified by dialysis in a dialysis bag (Mw=1000). Yield: 62%. ^{1}H-NMR($CDCl_3$, TMS, ppm): δ 6.65-6.69 (16H, 8aromatic ring), 7.54 (16H, 8aromatic ring), 8.11 (8H, s, 8-C*H*=N-), 3.62 (16H, 8-CH_2-C*H*$_2$-N=CH-), 3.51 (16H, 8-NH-C*H*$_2$-CH_2-N=C-), 3.23 (8H, 4-CONH-C*H*$_2$-CH2-N(-CH_2-)-CH_2-), 3.00 (48H, 8-N-(C*H*$_3$)$_2$), 2.80 (8H, 4 -C*H*$_2$-N(-CH_2-)-CH_2-), 2.64 (24H, 12-CH_2-N(-CH_2-) -C*H*$_2$-CH_2-) , 2.45 (4H, -CH_2-(-CH_2-)-N-C*H*$_2$-C*H*$_2$-N(-CH_2-)-CH_2-), 2.28 (24H, 12-C*H*$_2$-CO-). FT-IR: (KBr pellet, cm^{-1}): 3289; 3075; 2924; 2851; 1645; 1608; 1556; 1524; 1446; 1359; 1228; 1182; 1166.

PAMAM-PA G 2, G 3, G 4 and G 5 were synthesized in the same manner as PAMAM-PA G 1. Their spectroscopic characterizations were provided in Electronic Supplementary Material.

Synthesis of PAMAM Dendrimers Bearing 9-(3-bromopropyl)-9H-carbazole (PAMAM-Cz G 0, G 1, G 2, G 3 and G 4)

PAMAM-Cz G 0. 9-(3-Bromopropyl)-9H-carbazole was synthesized as shown in Scheme S-1. 9-(3-Bromopropyl)-9H-carbazole (0.060 g, 0.200 mmol) was added into the *N*, *N*-dimethylformamide (2 mL) solution of PAMAM dendrimer G 0 (0.020 g, 0.040 mmol), which was subsequently stirred at 30ºC for 12 h. The reaction mixture was dropwise added into diethyl ether (200 mL) and stirred for 24 h at room temperature. Upon filtrating, the solid residue was purified by dissolving in chloroform (30 mL) and evaporating the solvent under reduced pressure. The pale yellow colloidal precipitate was collected and further purified by dialysis in a dialysis bag (Mw= 1000). Yield: 45%. ^{1}H-NMR($CDCl_3$, TMS, ppm): δ 7.17-7.48 (64H, 8carbazole), 4.23 (16H, 8-CH_2-CH_2-CH_2-N-), 3.37-3.40 (8H, 4-CONH-CH_2-), 3.10 (8H, 4 -N(-CH_2-)-CH_2-), 2.78 (8H, 4-CH_2-N(-CH_2-)- CH_2-), 2.56 (8H, 4-CH_2-CO-), 2.43 (16H, 8-CH_2-CH_2-CH_2-N-) , 1.87 (16H, 8-CH_2-CH_2-CH_2-N-). FT-IR: (KBr pellet, cm^{-1}): 3361; 3259; 3051; 2924; 2852; 1658; 1597; 1548; 1463; 1454; 1348; 1327; 1234; 1216.

PAMAM-Cz G 1, G 2, G 3 and G 4 were synthesized in the same manner as PAMAM-Cz G 0. Their spectroscopic characterizations were provided in Electronic Supplementary Material.

The synthetic details and spectroscopic characterizations for PAMAM-P G 2, G 3, G 4, G 5 and PAMAM-Py G 0, G 1, G 2, G 3, G 4, G 5 were provided in Electronic Supplementary Material. The fluorescence spectra of PAMAM-PA G2 and PAMAM-PA G4 with different modification extents were provided in Electronic Supplementary Material (Figure S-8 and Figure S-9).

Results and Discussion

Fluorescence Monitoring of Chromophoric Modification of PAMAM Dendrimers

The small molecule 4-dimethylamino-benzaldehyde and macromolecular PAMAM dendrimers do not display any fluorescence emission. The former is due to the strong fluorescence quenching of the electron-accepting carbonyl groups. However, strong fluorescence was observed to increase gradually as PAMAM dendrimers were reacted with 4-dimethylaminobenzaldehyde as shown in Figure 1. The fluorescence intensity increases rapidly at the beginning of the macromolecular reaction of chromophoric modification, implying that the reaction proceeds rapidly at the early stage. Subsequently, the increase in intensity becomes slow. After about 80 min, the fluorescence intensity reaches a maximum, indicating that the reaction approaches its limit. Therefore, the fluorescence intensity can reflect the macromolecular reaction extents of the chromophoric modification of dendrimers.

To make sure the reliability of the fluorescence monitoring, the macromolecular reactions of chromophoric modifications were also monitored by ^{1}H-NMR

spectroscopy under the same condition as shown in Figure 2. The reaction extent could be calculated according to the increase in the NMR peak δ 8.1 ppm (assigned to -N=C*H*R).

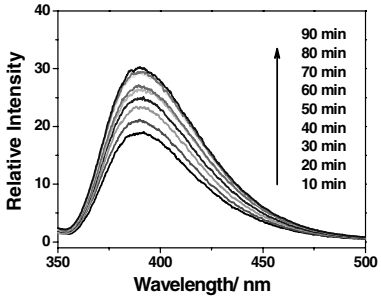

Figure 1. Changes in the fluorescence intensities during the reaction of PAMAM G 2 with 4-dimethylaminobenzaldehyde in methanol. λ_{ex}= 340 nm; reaction time for each spectrum from bottom to top: 10, 20, 30, 40, 50, 60, 70, 80, 90 min. [chromophore] = $5x10^{-6}$ M.

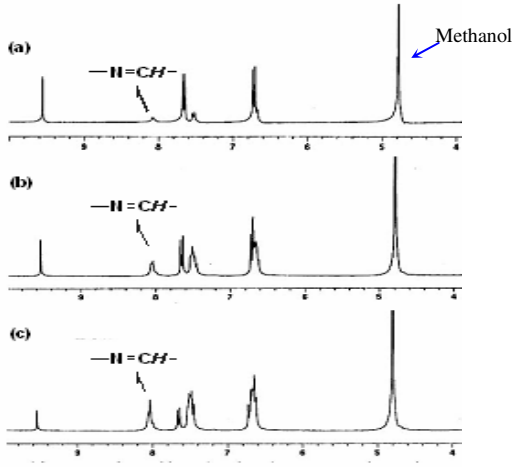

Figure 2. ^{1}H-NMR spectra during the reaction of PAMAM G 2 with 4 - dimethylamino-benzal-dehyde using methanol-d_4 as solvent; reaction time for each spectrum from top to bottom (min): 5 (a), 25 (b), 65 (c). The NMR peak at δ 8.1 ppm (-N=C*H*R) increases as the reaction proceeds.

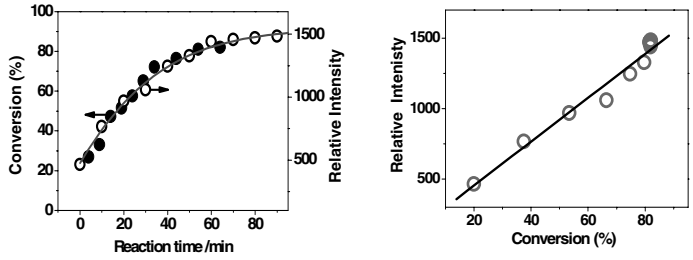

Figure 3. Left: reaction dynamics curves of PAMAM G 2 with 4-dimethylaminobenzaldehyde monitored by fluorescence (○) and ^{1}H-NMR spectroscopy (●). Right: correlation plot of fluorescence intensities versus reaction extents.

Figure 3 compares the reaction dynamic curves obtained from NMR data and that from fluorescence data. A linear correlation between fluorescence data and reaction extent was obtained as shown in Figure 3 (right), indicating that the macromolecular reactions of chromophoric modifications can be well monitored by fluorescence spectroscopy.

The increases in fluorescence intensities after chromophoric modifications of dendrimers were also observed for other generations and modified dendrimers PAMAM-Py, PAMAM-Cz, PAMAM-P (Figures S-1, S-2, S-3, S-4 in Electronic Supplementary Material). Therefore, the fluorescence monitoring is suitable for all the dendrimer systems given in this study. The fluorescence monitoring of chromophoric modification as a convenient and useful tool can be expected to play an important role in tailoring and optimizing the properties and related functions of dendrimers bearing chromophores. Compared with widely applied environment-sensitive fluorescence probe techniques, a distinct advantage of the fluorescence monitoring method is that it provides direct information on the conversion of chemical bonds.

Fluorescence Behavior of PAMAM Dendrimers Bearing Electron-donating Chromophores

For PAMAM dendrimers bearing carbazole groups (PAMAM-Cz), the absorption and emission peaks at 330 nm and 351 nm were observed in methanol. There is a little spectral overlap between the absorption and emission spectra (Figure S-5), indicating that the nonradiative energy transfer between chromophores is very weak. The same results were observed for PAMAM dendrimers modified with phenyl and pyrene groups at the periphery.

No evident changes in the fluorescence quantum yields were observed at the different generation of PAMAM-PA (Figure S-6 and Table S-1). The quantum yields of PAMAM-Cz G 0 to G 4 are 0.113, 0.115, 0.112, 0.128, 0.120, respectively, which are lower than that of small molecular carbazole (0.255). This could be attributed to the quenching effect of the dendritic backbone according to Pistolis and co-workers [18].

Solvent Effect

In general, fluorescence behaviors in various solvents with different polarity can reflect the interaction between the solvent and fluorophores, which can be described quantitatively by Lippert-Mataga equation [19, 20]:

$$\nu_a - \nu_f = (2/hc)\Delta f[(\mu_E - \mu_G)^2/a^3] + \text{constant}$$

$$\Delta f = (\varepsilon - 1)/(2\varepsilon + 1) - (n^2 - 1)/(2n^2 + 1)$$

where ν_a and ν_f are the wavenumbers (cm^{-1}) of the absorption and emission respectively. μ_E and μ_G are the dipole moments of ground state and excited state, respectively. Δf is a solvent parameter called as the orientation polarizability, which is a function of the refractive index (n) and dielectric constant (ε) of solvents.

The Stokes' shifts (ν_a-ν_f) of PAMAM-PA G 1 and PAMAM-P G 2 to G 4 in various solvents with different polarity (cyclohexane, dichloromethane, tetrahydrofuran, acetonitrile and *N*,*N*-dimethylformamide) were shown in Figure 4 and Table S-2. The Stokes' shifts increase gradually as the solvent parameters (Δf) increase, suggesting that the interaction between the solvents and the dendrimers is strengthened with

increasing the orientation polarizability (*Δf*), which in turn causes a decrease in the excited state energy of chromophores. This result also implies that solvent molecules can diffuse freely from the exterior to the interior of the modified dendrimers.

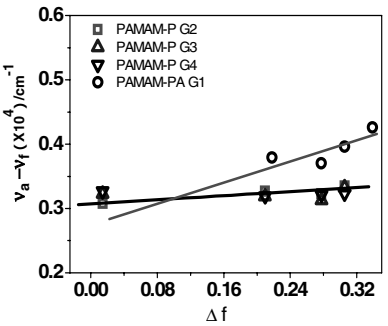

Figure 4. Plots of the Stokes' shifts (ν_a -ν_f) versus the solvent parameters (Δf) for PAMAM-PA G 1 and PAMAM-P G 2 to G 4.

PAMAM-P G 1 to G 4 display the same slope for the plots of the Stokes' shifts versus the orientation polarizability. PAMAM-PA G 1 displays a higher slope than that of PAMAM-P G 2. This may be attributed to the higher polarity of *N*, *N*-dimethylphenylamine (PA) groups than phenyl groups.

Fluorescence Quenching

To better understand the fluorescence behaviors of the modified dendrimers, a comparative and control experiment was designed. Specifically, the small molecular *N*, *N*-dimethylphenylamine (PA) was employed as a quencher to quench the fluorescence of macromolecular PAMAM-Py. For comparison, PAMAM-PA was employed as a macromolecular quencher to quench the fluorescence of small molecular pyrene (Py) in a control experiment as illustrated in Scheme 2.

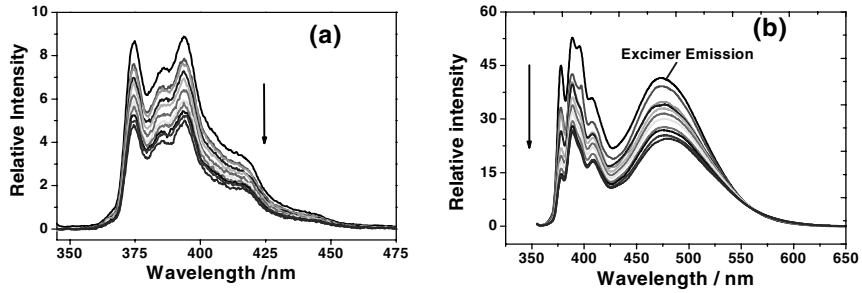

Figure 5. (a): Representative fluorescence spectra of pyrene (Py) with an addition of quencher PAMAM-PA G 5, λ_{ex}=334 nm, [Py]=1.0x10^{-6} M, [PAMAM-PA G5] (from top to bottom)= 0 , 6×10^{-6} , 12×10^{-6}, 18×10^{-6}, 24 ×10^{-6}, 30 ×10^{-6}, 36 ×10^{-6}, 42 ×10^{-6}, 48 ×10^{-6}, 54 ×10^{-6}, 60×10^{-6} M. (b): Fluorescence spectra of PAMAM-Py G 5 with an addition of quencher *N*, *N*-dimethylphenylamine (PA) in dichloromethane, λ_{ex}= 340 nm, [Py]=8.4x10^{-6} M, [PA] (from top to bottom) = 0, 1.24×10^{-6}, 2.88×10^{-6}, 3.78×10^{-6}, 5.03×10^{-6}, 6.30×10^{-6}, 7.57×10^{-6}, 8.82×10^{-5}, 1.01×10^{-5}, 1.13×10^{-5}, 1.27×10^{-5} M.

The kinetics of steady-state fluorescence quenching can be described by the Stern-Volmer equation [21]: $I_0/I = 1+ k_q\tau_0[Q]$ where I_0 and τ_0 are the unquenched intensity and lifetime, and [Q] is the quencher concentration. The quenched intensity (I) was corrected to avoid the inner filter effects due to the absorption of quenchers [22]. It is important to note that the correction for the quenched intensity is very necessary when the absorption of quenchers is close to the excitation wavelength. Some unreasonable results (e.g., $k_q >> 10^{10}$ M^{-1} s^{-1}) would be readily obtained if the data were not corrected [23].

In principle, the k_q value reflects the quenching efficiency or the accessibility of the quenchers to the fluorophores [21]. The fluorescence quenching spectra of the small molecular pyrene (Py) by macromolecular PAMAM-PA, and PAMAM-Py by PA were shown in Figure 5. Their Stern-Volmer plots and bimolecular quenching constants (k_q) were shown in Figure 6 and Figure 7, respectively.

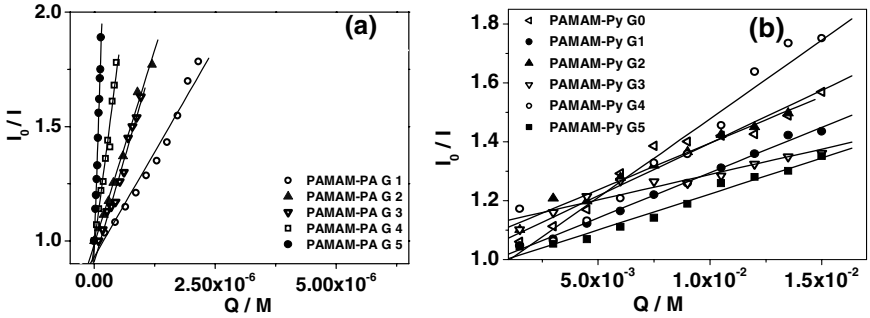

Figure 6. (a): Stern-Volmer plots for the fluorescence quenching of small molecular pyrene (Py) by macromolecular quencher (Q) PAMAM-PA G 1 to G 5; λ_{ex} =335 nm. (b): Fluorescence quenching of macromolecular PAMAM-Py G 0 to G 5 by small molecular quencher *N, N*-dimethylphenylamine (PA) in dichloromethane; λ_{ex}= 335nm.

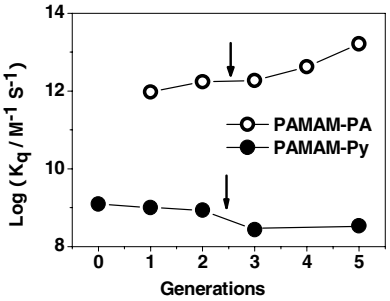

Figure 7. Bimolecular quenching constants (k_q) for the fluorescence quenching of pyrene (Py) by PAMAM-PA G 1 to G 5 and PAMAM-Py G 0 to G 5 by *N*, *N*-dimethylphenylamine (PA) in dichloromethane. The arrows indicate the architectural transitions of dendrimers occurring between G 2 and G 3.

For the fluorescence quenching of macromolecular PAMAM-Py by the small molecular PA, the k_q values decrease in the order of G 0 > G 1 > G 2 > G 3 > G 4, G 5 as shown in Figure 7. The k_q values of PAMAM-Py G 0 to G 2 are close to 10^9~10^{10} $M^{-1}s^{-1}$, indicating a diffusion-controlled quenching. This implies that the low

generations PAMAM-Py G 0 to G 2 adopt extended and open architectures, where the interior and exterior of dendrimers are accessible to the small molecular PA. With increasing generation of PAMAM-Py, the k_q value becomes small. This may be attributed to the steric hindrance at the higher generation. The higher generation PAMAM-Py tends to be a globular architecture with densely packed shells, which is more shielded from quenchers as illustrated in Scheme 2 (left).

Scheme 2. Schematic illustration for the fluorescence quenching of PAMAM-Py G 3 by *N*, *N*-dimethylphenylamine (PA) (left), where PAMAM-Py G 3 possesses a relatively compact Py shells and the quencher PA can not diffuse freely into the interior of dendrimers; and the fluorescence quenching of pyrene (Py) by PAMAM-PA G 3 (right), where PAMAM-PA G 3 possesses a less compact PA shells and the fluorophore Py can be encapsulated with a random distribution in the interior of dendrimers.

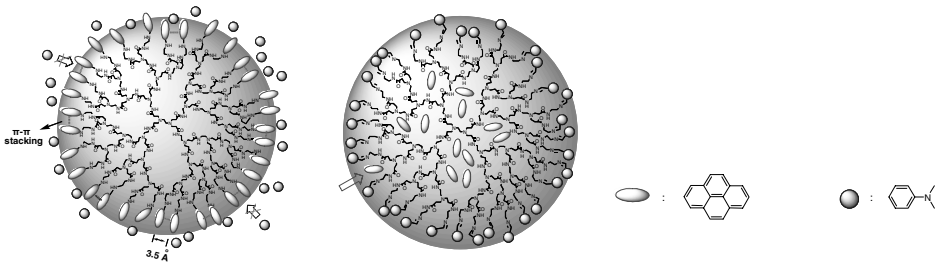

Interestingly, for the fluorescence quenching of the small molecular Py by macromolecular PAMAM-PA G 1 to G 5, the k_q values decrease in an opposite order (G5 > G4 > G3, G2 > G1) as shown in Figure 7. The k_q value for PAMAM-PA G 1 implies a diffusion-controlled quenching. This support the results obtained above, that is, the low generation dendrimers have a more extended conformation, which is readily accessible to the quenchers.

The k_q values (10^{12} $M^{-1}s^{-1}$) for PAMAM-PA G 3 to G 5 are two orders of magnitude higher than the values of diffusion-controlled quenching (10^{10} $M^{-1}s^{-1}$), indicating a static quenching for the high generation PAMAM-PA G 3 to G 5. This result can be explained from dendrimer architectures. The high generation dendrimers possess a globular architecture, thus can encapsulate and bind the small molecule Py like a "dendritic box" as described by Meijer [24], which leads to an effective static quenching as illustrated in Scheme 2 (right).

The comparative experiment looks like to give conflict results: (1) the high generation PAMAM-PA displays a high quenching efficiency due to its encapsulation effect. (2) However, the high generation PAMAM-Py displays a low quenching efficiency due to its steric shielding. In fact, a further analysis for the comparative study reveals interesting results, that is, the high generation PAMAM-Py possesses a more compact shell than the same generation PAMAM-PA. In the case of the high generation PAMAM-Py, the most of quenchers are shielded from the interior of dendrimers and cannot enter the interior due to the closely packed shell as shown in Scheme 2 (left). In contrast, the high generation PAMAM-PA has a less compact shell than the same generation PAMAM-Py. The quenchers can crowd into the interior of dendrimers, thus be encapsulated by dendrimers.

The interesting results can be further confirmed by the appearance of excimer emission of PAMAM-Py as shown in Figure 5 (b). The excimer emission was observed at 480 nm, indicating that partial Py chromophores tend to be parallelly packed each other with a distance of 3.5 Å as described by Crooks [6, 25]. In contrast, the excimer emission can not be observed for pyrene molecules as shown in Figure 5(a). This suggests that the pyrene chromophores dispersed randomly in the interior of the higher PAMAM-PA dendrimers as illustrated in Scheme 2 (right). In addition, the fluorescence quenching also reveals an architectural transition from the open and extended conformation to the closely packed conformation occurring between G 2 and G 3 as shown in Figure 7.

Electrochemical Properties

N, *N*-dimethylphenylamine chromophores are well known to be electron-active groups. Cyclic voltammetry is one of the most versatile electroanalytical techniques to study the properties of electron-active species [26]. In this work, cyclic voltammetric studies were carried out in acetonitrile using Bu_4NPF_6 (0.1 M) as supporting electrolyte and Ag/AgCl as an internal reference.

The cyclic voltammgrams of PAMAM-PA G 1 to G 5 in acetonitrile were provided in Electronic Supplementary Material (Figure S-7). PAMAM-PA G 1 to G 3 display almost the same oxidation potentials as shown in Figure 8 and Figure S-7, implying that they possess the same electron-donating ability. For the higher generation PAMAM-PA, the oxidation potentials decrease gradually with increasing the generation number (1.399 V (G 3), 1.263 V (G 4), 1.095 V (G 5)), indicating that the electron-donating ability increases at higher generations. This result indicates that the crowded PA groups of high generation dendrimers readily donate electrons. In addition, this result further reveals an architectural transition occurring at G 3.

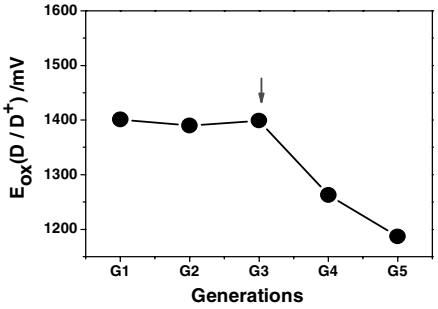

Figure 8. Oxidation potentials ($E_{ox}(D/D^+)$) of PAMAM-PA G 1 to G 5 obtained from cyclic voltammgrams in acetonitrile at scanning rate 50 mVs^{-1} (25 ºC).

In order to better understand the electrochemical properties, we measured the oxidation potentials of PAMAM-PA G 1 to G 5 at different scanning rates: 10, 20, 30, 40, 50, 70, 90 mv s^{-1}. Figure 9 (left) shows representative cyclic voltammgrams of PAMAM-PA G 1 at different scanning rates. The diffusion coefficients of PAMAM-PA G 1 to G 5 were calculated according to the Randales-Sevcik equation [27],

$$I_{pc}=2.69x10^5n^{3/2}A(D^{1/2}C)v^{1/2}$$

where A is the electrode surface area obtained from the reference ferrocene (0.01M) solution, n is the electron stoichiometry, D is the diffusion coefficient, C is the concentration, v is the scanning rate, and I_{pc} is the peak current. The anode oxidation of each PA group is one-step single electron oxidation process (n=1).

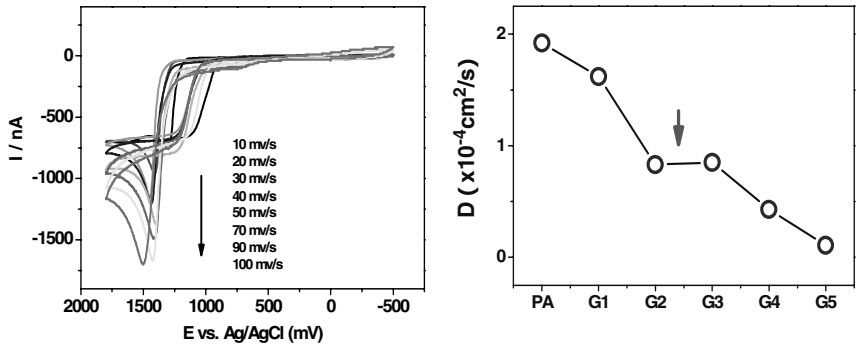

Figure 9. Left: representative cyclic voltammgrams of PAMAM-PA G 1 in acetonitrile (0.1M Bu_4NBF_6) at scanning rate 10, 20, 30, 40, 50, 70, 90, 100 mVs^{-1} (25 ºC). Right: diffusion coefficient of small molecular *N*, *N*-dimethylphenylamine (PA) and PAMAM-PA G 1 to G 5.

Figure 9 (right) shows that the diffusion coefficients decrease gradually with increasing generation number, suggesting that the size and shape of dendrimer increase with increasing the generation number. In the decreasing trend, a break point was observed between G 2 and G 3, implying a size and shape transition of dendrimers. Therefore, this electrochemical result further reveals the architectural transition of dendrimers from an extended structure to a globular structure occurring between G 2 and G 3.

Conclusion

Poly(amidoamine) dendrimers G 0 to G 5 were peripherally modified with photo- and electro-active *N*, *N*-dimethylphenylamine (PA), carbazole (Cz) and pyrene (Py) chromophores. Based on the fluorescence changes during macromolecular reaction of chromophoric modification of dendrimers, a fluorescence monitoring method was developed to monitor the reaction extents of dendrimers with chromophores. Compared with widely applied fluorescence probe techniques, a distinct advantage of the new fluorescence monitoring method is that it can provide direct information on the conversion of chemical bonds during dendrimer reaction without a contaminated addition of small molecules. The reliability of the fluorescence monitoring method was confirmed by NMR spectroscopy. The fluorescence monitoring for the chromophoric modification of dendrimers can be expected to play an important role in tailoring and optimizing the dendrimer properties and related functions. The fluorescence quenching of PAMAM-Py by small molecular quencher PA and fluorescence quenching of pyrene by macromolecular quencher PAMAM-PA were investigated respectively. A comparative study reveals that the high generation PAMAM-Py possesses a relatively compact Py shell as compared with the same generation PAMAM-PA. The fluorescence quenching of small molecular Py by high generation PAMAM-PA is a static quenching process due to the encapsulation effect

of dendrimers. Electrochemical studies further reveal that an architectural transition occurs between G 2 and G 3, and the electron-donating ability of PAMAM-PA G 3 to G 5 increases with increasing the generation number.

Acknowledgements. We are most grateful to the National Natural Science Foundation of China (NSFC Grant No. 20340420002 and No. 20374002) for the financial support, and partial support from the Nanotechnology Institute of Southeastern Pennsylvania.

References and Notes

1. Grayson SM, Fréchet JMJ (2001) Chem Rev 101: 3819-3868.
2. Vicinelli V, Ceroni P, Maestri M, Balzani V, Gorka M, Vogtle F (2002) J Am Chem Soc 124: 6461-6468.
3. Tsuda K, Dol GC, Gensch T, Hofkens J, Latterini L, Weener JW, Meijer EW, De Schryver FC (2000) J Am Chem Soc 122: 3445-3452.
4. Adronov A, Gilat SL, Frechet JMJ, Ohta K, Neuwahl FVR, Fleming GR (2000) J Am Chem Soc 122:1175-1185.
5. Yeow EKL, Ghiggino KP, Reek JNH, Crossley MJ, Bosman AW, Schenning APHJ, Meijer EW (2000) J Phys Chem B 104: 2596-2606.
6. Baker LA, Crooks RM (2000) Macromolecules 33: 9034-9039.
7. Stewart GM, Fox MA (1996) J Am Chem Soc 118: 4354-4360.
8. Storrier GD, Takada K, Abruna HD (1999) Langmuir 15: 872-884.
9. Yang L, Luo Y, Jia X, Ji Y, You L, Zhou Q (2004) J Phys Chem B 108: 1176-1178.
10. Wang J, Chen J, Jia X, Cao W, Li M (2000) Chem Comm 511-512.
11. Zhong H, Wang J, Jia X, Li Y, Qin Y, Chen J, Zhao XS, Cao W (2001) Macromol Rapid Commun 22: 583-586.
12. Wang BB, Zhang X, Jia XR, Li ZC, Ji Y, Yang L, Wei Y (2004) J Am Chem Soc 126: 15180-15194.
13. Kim YS, Sook C, Sung P (1995) J Appl Polym Sci 57(3): 363-370.
14. Pekcan O, Yilmaz Y, Okay O (1997) Polymer 38(7): 1693-1698.
15. (a) Aspee A, Garcia O, Maretti L, Sastre R, Scaiano JC (2003) Macromolecules 36: 3550-3556, (b) Ballesteros OG, Maretti L, Sastre R, Scaiano JC (2001) Macromolecules 34: 6184-6187.
16. Grebel-Koehler D, Liu D, De Feyter S, Enkelmann V, Weil T, Engels C, Samyn C, Mullen K, De Schryver FC (2003) Macromolecules 36: 578-590.
17. (a) Tomalia DA, Baker H, Dewald J, Hall M, Kallos G, Martin S, Roeck J, Ryder J, Smith P (1985) Polym J 17: 117-132. (b) Santo M, Fox MA (1999) J Phys Org Chem 12: 293-307.
18. Pistolis G, Malliaris A, Paleos CM, Tsiourvas D (1997) Langmuir 13: 5870-5875.
19. Von Lippert V (1957) Electrochemistry 61: 962-975.
20. Mataga N, Kaifu Y, Koizumi M (1956) Bull Chem Soc Jpn 29: 465-470.
21. Lakowicz JR (1999) Principles of Fluorescence Spectroscopy, 2nd ed., Plenum Press: New York, p 239.
22. To avoid the inner filter effects due to the absorption of the incident light and the emitted light, the fluorescence intensity was corrected as follow: $I = I_{ob} \times 10^{[(ODex+ODem)/2]}$. I_{ob} is the observed fluorescence intensity. OD_{ex} and OD_{em} are the optical densities at excitation and emission wavelength, respectively.
23. Phelan JC, Sung CSP (1997) Macromolecules 30: 6845-6851.
24. Jansen JFGA, de Brabander-van den Berg EMM, Meijer EW (1994) Science 266: 1226-1229.
25. Winnik FM (1993) Chem Rev 93: 587-614.
26. Zhang X, Li ZC, Li KB, Du FS, Li FM (2004) J Am Chem Soc 126: 12200-12201.
27. Asakawa T, Sunagawa H, Miyagishi S (1998) Langmuir 14: 7091-7094.